

# Early intervention and lifelong treatment with GLP1 receptor agonist liraglutide in a Wolfram Syndrome rat model with an emphasis on visual neurodegeneration, sensorineural hearing loss and diabetic phenotype

Toomas Jagomäe (✉ [toomas.jagomae@gmail.com](mailto:toomas.jagomae@gmail.com))

University of Tartu: Tartu Ülikool <https://orcid.org/0000-0002-2863-4844>

**Kadri Seppa**

University of Tartu: Tartu Ülikool

**Riin Reimets**

Tartu Ülikool: Tartu Ülikool

**Marko Pastak**

Tartu University Hospital: Tartu Ülikooli Kliinikum

**Mihkel Plaas**

Tartu University Hospital: Tartu Ülikooli Kliinikum

**Miriam A Hickey**

University of Tartu: Tartu Ülikool

**Kaia Grete Kukker**

University of Tartu: Tartu Ülikool

**Lieve Moons**

KU Leuven: Katholieke Universiteit Leuven

**Lies De Groef**

KU Leuven University: Katholieke Universiteit Leuven

**Eero Vasar**

University of Tartu: Tartu Ülikool

**Allen Kaasik**

University of Tartu: Tartu Ülikool

**Anton Terasmaa**

KBFI: Keemilise ja Bioloogilise Fuusika Instituut

**Mario Plaas**

University of Tartu: Tartu Ülikool

**Keywords:** Wolfram syndrome, Wfs1, GLP1 receptor agonist, liraglutide, rat model, neurodegeneration, optic nerve atrophy, hearing loss, visual acuity, diabetes

**Posted Date:** September 23rd, 2021

**DOI:** <https://doi.org/10.21203/rs.3.rs-903256/v1>

**License:**  This work is licensed under a Creative Commons Attribution 4.0 International License.

[Read Full License](#)

---

**Version of Record:** A version of this preprint was published at Cells on November 16th, 2021. See the published version at <https://doi.org/10.3390/cells10113193>.

# Early intervention and lifelong treatment with GLP1 receptor agonist liraglutide in a Wolfram Syndrome rat model with an emphasis on visual neurodegeneration, sensorineural hearing loss and diabetic phenotype

Toomas Jagomäe<sup>1,5\*</sup>, Kadri Seppa<sup>1</sup>, Riin Reimets<sup>1</sup>, Marko Pastak<sup>2</sup>, Mihkel Plaas<sup>3</sup>, Miriam A. Hickey<sup>4</sup>, Kaia Grete Kukker<sup>1</sup>, Lieve Moons<sup>6</sup>, Lies De Groef<sup>6</sup>, Eero Vasar<sup>5</sup>, Allen Kaasik<sup>4</sup>, Anton Terasmaa<sup>1</sup> and Mario Plaas<sup>1,5\*</sup>

<sup>1</sup> Institute of Biomedicine and Translational Medicine, Laboratory Animal Centre, University of Tartu, 14B Ravila Street, Tartu 50411, Estonia

<sup>2</sup> Eye Clinic of Tartu University Hospital, L. Puusepa 8 Street, Tartu, 50406, Estonia

<sup>3</sup> Ear Clinic of Tartu University Hospital, L. Puusepa 1a Street, Tartu, 50406, Estonia

<sup>4</sup> Department of Pharmacology, Institute of Biomedicine and Translational Medicine, University of Tartu, 19 Ravila Street, Tartu 50411, Estonia

<sup>5</sup> Institute of Biomedicine and Translational Medicine, Department of Physiology, University of Tartu, 19 Ravila Street, Tartu 50411, Estonia

<sup>6</sup> Department of Biology, University of Leuven, Research Group Neural Circuit Development and Regeneration, Naamsestraat 61, box 2464, 3000 Leuven, Belgium & Leuven Brain Institute, 3000 Leuven, Belgium

\*To whom correspondence should be addressed:

Mario Plaas, Institute of Biomedicine and Translational Medicine, University of Tartu, 19 Ravila Street, Tartu 50411, Estonia. Phone: +372 502 3056, E-mail: [mario.plaas@ut.ee](mailto:mario.plaas@ut.ee)

Email addresses: [mario.plaas@ut.ee](mailto:mario.plaas@ut.ee); [toomas.jagomae@gmail.com](mailto:toomas.jagomae@gmail.com); [kadri.seppa@ut.ee](mailto:kadri.seppa@ut.ee); [riin.reimets@ut.ee](mailto:riin.reimets@ut.ee); [marko.pastak@kliinikum.ee](mailto:marko.pastak@kliinikum.ee); [miriam@ut.ee](mailto:miriam@ut.ee); [lies.degroef@kuleuven.be](mailto:lies.degroef@kuleuven.be); [lieve.moons@kuleuven.be](mailto:lieve.moons@kuleuven.be); [kaiagretekukker@gmail.com](mailto:kaiagretekukker@gmail.com); [anton.terasmaa@kbfi.ee](mailto:anton.terasmaa@kbfi.ee); [eero.vasar@ut.ee](mailto:eero.vasar@ut.ee); [mihkel.plaas@kliinikum.ee](mailto:mihkel.plaas@kliinikum.ee); [allen.kaasik@ut.ee](mailto:allen.kaasik@ut.ee)

## Abstract

**Background:** Wolfram syndrome (WS), also known as a DIDMOAD (Diabetes Insipidus, early-onset Diabetes Mellitus, Optic nerve Atrophy and Deafness) is a rare autosomal disorder caused by mutations in the *Wolframin1* (*WFS1*) gene. Previous studies revealed that glucagon-like peptide-1 receptor agonist (GLP1 RA) anti-diabetic drugs are effective in delaying and restoring glucose control in WS animal models and patients. The GLP1 RA liraglutide has also been shown to have neuroprotective properties in aged WS rats, reducing neuroinflammation, retinal ganglion cell death and optic nerve degeneration.

WS is an early-onset, chronic condition and, therefore, early diagnosis and lifelong pharmacological treatment is the best solution to control disease progression in WS patients. Hence, the aim of this study was to evaluate the efficacy of the long-term liraglutide treatment on progression of WS symptoms. For this purpose, 2-month-old WS rats were treated with liraglutide (0.4mg/kg/day) up to the age of 18 months and changes in diabetes markers, visual acuity, hearing sensitivity were monitored *in vivo* over the course of the 16-month treatment period.

**Results:** Early and chronic (16-month) intervention with the GLP-1 RA liraglutide delayed the development of glucose intolerance in WS rats. At the end of the experiment, 91% of saline- and 55% of liraglutide-treated WS rats needed daily insulin supplementation. Liraglutide administration was effective in maintaining visual acuity in WS rats by stalling the progression of cataract, degeneration of retinal ganglion cells and of optic nerve atrophy. Prolonged liraglutide therapy could not prevent sensorineural hearing loss at low frequencies.

**Conclusion:** The rat model of WS used in this study is an excellent predictive model for preclinical trials as it closely recapitulates the relative onset and severity of the main symptoms of WS observed in human patients. We found that a 16-month treatment with GLP1 receptor

agonist liraglutide delays or prevents the onset of diabetes and protects against vision loss in a rat model of Wolfram syndrome. Therefore, early diagnosis and prophylactic treatment with the GLP-1R agonist liraglutide may also prove to be a promising treatment option for Wolfram syndrome patients by increasing the quality of life of WS patients.

### **Keywords**

Wolfram syndrome, Wfs1, GLP1 receptor agonist, liraglutide, rat model, neurodegeneration, optic nerve atrophy, hearing loss, visual acuity, diabetes

## Introduction

Wolfram syndrome (WS) is a rare autosomal recessive disorder caused by mutations in the Wolframin 1 (*WFS1*) gene. The syndrome first manifests as diabetes mellitus, followed by optic nerve atrophy, deafness and neurodegeneration (Barrett and Bunday, 1997; Barrett et al., 1997; Rigoli et al., 2011). Prevalence, severity and emergence of the symptoms depends on the genetic background and location of the mutations rendering dysfunction of the WFS1 protein (Bueno et al., 2018; Chausseot et al., 2011; Duan et al., 2018; Wilf-Yarkoni et al., 2021). In WS patients, diabetes is effectively managed, leaving loss of vision and neurodegeneration the main symptoms impairing quality of life (Urano, 2016). Thus, the development and evaluation of neuroprotective strategies is of utmost importance from the patient's perspective.

The *WFS1* gene encodes an 890 amino acid long transmembrane protein (WFS1 or Wolframin) that is localized on the endoplasmic reticulum (ER) membrane and in the secretory granules (Gharanei et al., 2013; Urano, 2016). WFS1 protein is highly expressed in the heart, lungs, placenta, pancreas, inner ear, specific regions of the brain (Luuk et al., 2008; Strom et al., 1998; Suzuki et al., 2018), and in the retina (Bonnet et al., 2014). Its exact function remains elusive, but elevated endoplasmic reticulum (ER) stress, dysregulation of intracellular calcium metabolism (Fonseca et al., 2005; Takei et al., 2006) and dysfunction of mitochondria (Cagalinec et al., 2016; Delprat et al., 2018) are cellular events connected with functional *WFS1* deficiency.

A *Wfs1* deficient rat model of WS (*Wfs1* KO) was recently constructed and validated at the University of Tartu (Plaas et al., 2017). *Wfs1* KO rats develop a more prominent diabetic phenotype than any previously generated mouse model of WS and show neurodegeneration of the brainstem and optic nerve. As such, this rat model of WS recapitulates clinical findings observed in human patients and therefore provides an excellent model to evaluate

pharmacological treatment strategies (Plaas et al., 2017; Seppa et al., 2019, 2021; Toots et al., 2018).

Previous studies revealed GLP1 receptor agonists (GLP1 RA) to be effective in restoration of glucose control in genetic mouse (Kondo et al., 2018; Sedman et al., 2016) and rat (Toots et al., 2018) models of WS. Moreover, treatment with the GLP1 RA liraglutide provided neuroprotective and anti-inflammatory effects in old *Wfs1* KO rats by restricting the progression of optic nerve atrophy and reducing glial activation (Seppa et al., 2019, 2021).

WS is a lifelong condition and, therefore, any pharmacological treatment of WS patients will also be lifelong. GLP1 receptor agonist treatment is currently the only known treatment strategy that was shown to be effective in several animal models of WS and in human patients (Kondo et al., 2018; Scully and Wolfsdorf, 2020). However, the long-lasting effect of such treatment has never been evaluated. Hence, the aim of this study was to evaluate the safety and efficacy of long-term, prophylactic GLP1 RA treatment in a rat model of WS. For this purpose, changes in diabetes markers, visual acuity and hearing sensitivity were monitored *in vivo* during the course of a 16-month treatment period with liraglutide. We found that administration of a GLP-1R agonist before the onset of WS symptoms evidently postponed the main symptoms of WS, development of glucose intolerance and vision loss.

## Materials and Methods

### Animals

All experimental protocols were approved by the Estonian Project Authorisation Committee for Animal Experiments (No 138, 18th of March 2019), and all experiments were performed in accordance with the European Communities Directive of September 2010 (2010/63/EU).

Generation and phenotype of a Wfs1 mutant (Wfs1-ex5-KO232, Wfs1 KO) rat has been described previously (Plaas et al., 2017). Breeding and genotyping were performed at the Laboratory Animal Centre at the University of Tartu. For this study, male homozygous Wfs1-deficient (Wfs1 KO) and littermate control rats (WT) were used. The animals were housed in cages in groups of 2–4 animals per cage under a 12-h light/dark cycle (lights on at 7 a.m.). To minimize retinal phototoxicity, animals were maintained at dim light conditions (60 – 80 lux). Rats had unlimited access to food and water except during testing. Sniff universal mouse and rat maintenance diet (Sniff #V1534) and reverse osmosis-purified water were used. Experiments were performed between 9 a.m. and 5 p.m.

### Long-term (prolonged) treatment with GLP1 receptor agonist liraglutide

Animals were 2-months-old at the start of the treatment and randomly divided into four experimental groups with at least 20 animals in each group: wild type animals with saline treatment (WT Sal), n = 23; wild type animals with liraglutide treatment (WT Lira), n = 20; Wfs1 KO animals with saline treatment (KO Sal), n = 27; Wfs1 KO animals with liraglutide treatment (KO Lira), n = 24. The liraglutide-treated animals received 0.4 mg/kg liraglutide (Novo Nordisk, Denmark), and the control groups received a 0.9% NaCl solution (saline). Injections of 1 ml/kg volume were made subcutaneously once a day, between 8 and 11 a.m., for 16 months.

Rats were weighed once a week, and their base blood sugar level was measured once a month from the tail vein using a handheld glucometer (Accu-Check Go, Roche, Germany). In order to avoid hyperglycemia-induced symptoms, supportive insulin treatment (100 IU/ml, Levemir, Novo Nordisk, Denmark) was initiated in hyperglycemic Wfs1 KO rats. Animals with a basal blood glucose level of 10 mmol/L received 1 IU/kg insulin twice per day by subcutaneous injections. Every subsequent 5 mmol/L increase of blood glucose level, the given insulin dose was increased by 1 IU/kg (i.e. animals with a blood glucose level of 20 mmol/L received 6 IU/kg insulin twice per day) (Luippold et al., 2016; Nordquist and Sjöquist, 2009)

As expected in such a prolonged treatment study, some animals were lost during the experiment or had to be sacrificed for ethical reasons. The number of animals lost in each group was: 7 out of 23 in WT SAL; 7 out of 27 in KO SAL; 8 out of 20 in WT LIRA and 4 out of 24 in KO LIRA. In the vast majority of cases, the cause of death of WT animals was cancer, which is a common trait of Sprague-Dawley rats (Chandra et al., 1992). The majority cause of death of KO animals was uncontrollable diabetes mellitus. In two cases, the cause of death was unknown.

### **Intraperitoneal glucose tolerance tests (IPGTT)**

Animals were deprived of food for 3 h before and during the experiment; water was available throughout the experiment. Glucose (Sigma-Aldrich) was dissolved in 0.9% saline solution (20% w/vol) and administered intraperitoneally at a dose of 2 g/kg of body weight. Blood glucose levels were measured at the indicated time points from the tail vein using a hand-held glucometer (Accu-Check Go, Roche, Mannheim, Germany), immediately before and 30 min after glucose administration. Samples were used for insulin (CrystalChem cat# 90060), c-peptide (CrystalChem cat# 90055) and glucagon (CrystalChem cat# 81519) measurements

using ELISA tests. For serum separation, blood was allowed to clot, centrifuged for 15 min at 2000x g, and stored at -80° C until further analysis.

IPGTT was performed at the beginning of experiment before the drug treatment (age 2 months) and at the ages of 7.5 and 11.5 months. To minimize the possible acute effects of drug treatment, the IPGTT experiment was performed 24 hours after administration of liraglutide or vehicle.

### **2-hour postprandial blood sugar test**

In order to measure postprandial blood glucose levels rats were deprived for food for 3 hours and blood glucose levels were measured from tail vein using glucometer (Accu-Check Go, Roche, Mannheim, Germany). Subsequently blood glucose levels were measured 2 hours after the animals had access to food.

### ***In vivo* magnetic resonance imaging**

In vivo magnetic resonance imaging (MRI) imaging was performed at the ages of 17 months as described previously by our group (Plaas et al., 2017). For the optic nerve + chiasm + tract, segmentation began where the optic nerves emerged through the optic canal foramina and continued until the point where the optic tract was no longer discernable from surrounding parenchyma.

### **Hearing evaluation**

Hearing was evaluated by measuring otoacoustic emissions (OAE). OAE-s reflect the function of outer hair cells (Kemp, 1978) and are widely used as a hearing loss screening method in every day clinical practice (Kemp, 2002). A commercial clinical instrument (Sentiero Diagnostics, PATH medical GmbH) with frequency modulated distortion product otoacoustic emission (DPOAE) tympanometry upgrade (FMDPOAETM) was used to measure DPOAEs. DPOAE FULL test protocol was used, including enabled automated background noise

calibration, automated threshold detection algorithm and automatic scissor paradigm options. The F2 frequencies were 1, 1.5, 2, 3, 4, 5, 6, 8 kHz. Stimulus level L2: 25 to 65 dB SPL, step 5dB (automated threshold detection algorithm). L2/L1 relation was adjusted automatically by the device software. Cochlear hearing levels were estimated from measured DPOAE-s at distinct hearing frequencies using a pre-set software protocol by the manufacturer (Pathme GmbH whitepaper). Rats were tested at the age of 2, 6.5, 11.5 and 17 months and all tested ears were inspected visually to rule out potential causes for conductive hearing loss (cerumen, inflammation, fluids etc) as DPOAE-s cannot distinguish between conductive and sensorineural hearing loss. During the procedure, rats were anesthetized using isoflurane (for induction 3% of and for anesthesia maintenance 1,5% isoflurane was used, flow speed 2 l/min medical oxygen). To avoid anesthesia effects on cochlear outer hair cell and cochlear amplifier function, only the right ear was tested first and animals were woken up (Sheppard et al., 2018). After one hour wash out period, the procedure was repeated to measure the left ear. The average of right and left ear readings was used for analysis. It should be emphasized that DPOAEs only reflect outer hair cell functionality and therefore are not present at a hearing loss higher 50 dB HL. Therefore hearing loss greater than 50dB in any given frequency is estimated by the software (Pathme GmbH Whitepaper).

### **Visual acuity analysis**

To measure visual acuity, a virtual optomotor task (OptoMotry©, Cerebral Mechanics Inc) was used and the test was performed as described previously (Seppa et al., 2021). Shortly, animals were placed in the center of a virtual rotating cylinder displaying vertical bars. The width of the bars was made progressively smaller and the tracking behavior of the animals was recorded. The minimal width of the bars that induced tracking behavior is a surrogate measure of the maximal spatial frequency resolution of the rat. Clockwise rotation was detected by the left eye and anti-clockwise rotation by the right eye. Visual acuity data are presented as the mean of

clockwise and anti-clockwise testing. Visual acuity was evaluated at the ages of 8.5, 12.5 and 17 months.

### **Cataract scoring**

Lens changes, monitored by a portable slit lamp following dilation with 1% Tropicamide, were evaluated by a trained ophthalmologist blinded to the experimental protocol, as described previously (Livesey et al., 1995). Severity of cataract was scored as follows: 0, clear; 1, posterior subcapsular (PSC) haze; 2, spokes, suture enhancement and powdery PSC deposits; 3, prominent PSC punctate opacities with spokes and suture enhancement; 4, PSC opacity blocks appearance of retinal vessels; 5, start of cortical involvement; and 6, total lens opacity visible with naked eye. The mean of both eyes cataract scores was calculated and presented. Cataract scores were evaluated at the age of 13 and 17 months.

### **Intraocular pressure scoring**

Intraocular pressure (IOP) was measured using an Icare TONOLAB device that is specially designed for small rodent (rat/mouse) IOP measurements. During the procedure, rats were anesthetized using isoflurane (induction: 3%; maintenance: 1.5%; flow speed 2 l/min medical oxygen). The IOP for both eyes was measured following the manufacturer's test protocol. The mean IOP values for both eyes was calculated and presented. IOP was measured at the age of 17 months.

### **Tissue collection and preparation**

Rats were deeply anesthetized using a mixture of ketamine (100 mg/kg i.p.) and dexmedetomidine (0.5 mg/kg i.p.) until loss of reflexes. Blood samples (about 10 ml each) was taken via cardiac puncture and thereafter animals were transcardially perfused with 0.1 M phosphate buffer (PB: 100 mM Na<sub>2</sub>HPO<sub>4</sub>, 100 mM NaH<sub>2</sub>PO<sub>4</sub>, pH 7.4) followed by 4% paraformaldehyde in PB (100 mM Na<sub>2</sub>HPO<sub>4</sub>, 100 mM NaH<sub>2</sub>PO<sub>4</sub>, pH 7.2; 300ml/5 min). Tissues

of interest were dissected and immersion fixed in 4% PFA/PBS (PBS, 150 mM NaCl, 36 mM Na<sub>2</sub>HPO<sub>4</sub>, 14 mM NaH<sub>2</sub>PO<sub>4</sub>, pH 7.4) overnight at 4°C. The PFA solution was decanted and then replaced with fresh PBS supplemented with 0.01% sodium azide, this solution was changed once daily for a period of three days. Thereafter, tissues were cryoprotected in 30% sucrose/PBS solution for 4-5 days at 4°C with gentle agitation. Tissues were then frozen by immersing in isobutane cooled to -40°C and kept at -80°C until further use.

Optic nerves were carefully removed and the right optic nerve was processed and stored as described above. The left optic nerve was immersion fixed in 2% glutaraldehyde/160 mM sucrose/90 mM sodium cacodylate in water and kept over 24 hours at 4°C for electron microscopy analysis.

### **Retinal wholemount immunohistochemistry**

After perfusion, one eye from each animal was enucleated and immersed in 1% PFA/PBS for 12 hours and subsequently washed at least 3 times with PBS over 3 days. Retinas were then dissected and kept in PBS until further use. Retinal ganglion cells were visualized and counted via immunostaining for the POU-domain transcription factor Brn3a that is specifically expressed in retinal ganglion cells (Nadal-Nicolás et al., 2009), as previously described in detail by Geeraerts et al., 2016. Analyses were performed on eight frames, randomly selected in the mid-peripheral and peripheral retina, with a total area of 122601  $\mu\text{m}^2$  per retinal wholemount (5-6 animals per condition), and the number of Brn3a positive cells per  $\text{mm}^2$  was calculated.

### **Electron microscopy**

After the immersion fixation, the optic nerves from each animal (n=7-9) were incubated at 4°C until further washing with 90 mM Na-cacodylate buffer with subsequent processing as described previously (Seppa et al., 2021). Electron micrographs for analysis were collected using an Orius SC200B CCD camera (Gatan Inc.) mounted on a Tecnai G<sup>2</sup> Spirit

TWIN/BioTWIN transmission electron microscope (FEI, Netherlands). Representative figures for illustrations were collected using a side mounted Veleta CCD camera (Olympus).

### **Morphometric evaluation of optic nerve fibers**

Morphometric analysis of optic nerve fibers was performed on 35.1756  $\mu\text{m}$  (width) x 23.4504  $\mu\text{m}$  (height) images (pixel size: 0.0458x0.0458  $\mu\text{m}^2$ ) using ImageJ software version 1.53c (Schindelin et al., 2012). Cross-sections of optic nerves were divided into 10–11 non-overlapping random regions to minimize the variation in fiber size distributions. Five fields of view were randomly selected for analysis and on average 1400 nerve fibers were counted from individual rats (7 - 9 animals for each group). Only fibers whose contour was completely within field of view were counted.

Axon area measurements were performed on scale reduced images (scale: x=0.1918, y=0.1918). Average axon area per field of view was calculated as the sum of the individual axon areas per field of view. Average myelin areas were measured as the area of grayscale from converted to black, on 8-bit images (threshold 1-255). An area-based g-ratio (axon area divided by axon area plus myelin area) was calculated. The methods for counted degenerating fiber abnormalities were described previously (Seppa et al., 2021).

### **Data analysis**

GraphPad Prism version 9 software (GraphPad Software Inc., San Diego, CA, USA) was used for statistical analysis, and  $p < 0.05$  was considered statistically significant. The data are presented as mean  $\pm$  SEM and were compared using repeated measures ANOVA followed by Bonferroni's multiple comparisons test or the data were compared using one- or two-way ANOVA followed by Tukey's multiple comparisons test.

## Results

### A 16-month treatment with liraglutide delays the onset of diabetes in a rat model of Wolfram syndrome

Previously we have shown that a 5-month preventive treatment with liraglutide, starting before the onset of WS symptoms, protected against the development of glucose intolerance in Wfs1 KO rats (Toots et al., 2018). Whether liraglutide prevents or only delays diabetes in Wfs1 KO rats is still unknown, thus the aim of this study was to investigate if long-term, preventive treatment, is able to stop the development of diabetes.

First, body weight changes were monitored over time. Liraglutide treatment induced a slight reduction of body weight during the first week of administration in WT and Wfs1 KO animals (Figure 1a), in agreement with our previous work using GLP1 receptor agonists in this rat model of WS (Seppa et al., 2019, 2021; Toots et al., 2018).

Next, to monitor glucose tolerance over time, intraperitoneal glucose tolerance tests (IPGTT) were performed at the age of 2, 7.5 and 11.5 months. At the age of 2 months, there were no differences between the experimental groups (Figure 1b, c). At the age of 7.5 months, saline-treated Wfs1 KO rats had developed glucose intolerance, which was confirmed by an area-under-the-curve analysis ( $p < 0.0001$ ) (Figure 1b, d). Liraglutide treatment prevented the development of diabetes in 63% of Wfs1 KO animals ( $p < 0.0001$ ) (Figure 1b, e). By 11.5 months of age, 62.5% of liraglutide-treated Wfs1 KO animals remained diabetes-free ( $p < 0.0001$ ) (Figure 1b) whereas glucose intolerance increased ( $p < 0.0001$ ) in saline-treated Wfs1 KO rats (Figure 1b, e).

To assess the responsiveness of pancreatic islet cells to a glucose challenge, serum c-peptide, insulin and glucagon levels were measured before and 30 minutes after administration of glucose in the IPGTT at the age of 2, 7.5 and 11.5 months. At the age of 2 months, there were

no differences between experimental groups (Figure 2 a-c). At the age of 7.5 months, Wfs1 KO rats show the first signs of diabetes by reduced c-peptide (Figure 2d) and insulin (Figure 2e), and increased glucagon secretion ( $p < 0.01$ ) (Figure 2f). Liraglutide treatment prevented these changes (p-value?). At the age of 11.5 months, Wfs1 KO rats were not able to secrete c-peptide (Figure 2g) nor insulin (Figure 2h) and their glucagon levels were increased ( $p < 0.001$ ) (Figure 2i). Liraglutide-treated Wfs1 KO rats remained capable of secreting c-peptide ( $p < 0.05$ ) (Figure 2g).

At 9 months of age, saline-treated Wfs1 KO animals started to lose weight (Figure 1a) and develop hyperglycemia (Figure 1f), indicating the onset of diabetes. To prevent complications due to diabetes, supportive treatment with insulin was initiated in 12-month-old Wfs1 KO animals (Figure 1g). At 17 months of age, only 55% of the liraglutide-treated Wfs1 KO animals required supportive insulin treatment, whereas 90% of the saline-treated Wfs1 KO animals needed supportive insulin. Additionally, the insulin dose for saline-treated Wfs1 KO rats was higher than in liraglutide-treated Wfs1 KO animals ( $p < 0.05$ ) (Figure 1g). At the age of 16 months, most of the Wfs1 KO animals had developed hyperglycaemia (Figure 1f), therefore it was not ethical to perform IPGTT. Hence, a 2-hour postprandial blood sugar test was performed, showing that the blood sugar test results did not differ between treatment groups of Wfs1 KO animals. Thus, we can conclude that liraglutide treatment delays but does not prevent the development of diabetes in Wfs1 KO rats.

### **Liraglutide treatment did not prevent progressive sensorineural hearing loss of Wfs1 KO rats**

Sensorineural hearing loss in WS patients is highly prevalent therefore we sought to evaluate the hearing sensitivity in WS rats during the course of liraglutide treatment. Cochlear hearing levels were estimated by DPOAE-s at the age of 2, 6.5, 11 and 17 months. At the age of 2

months, hearing sensitivity was indistinguishable between experimental groups (Figure 3a). At the age of 6.5 months, hearing sensitivity of Wfs1 KO rats started to decline from 2 kHz ( $p < 0.0001$ ) to 5 kHz ( $p < 0.05$ ) (Figure 3b), compared to saline-treated WT rats. The estimated hearing loss further progressed by the age of 17 months both in terms of estimated hearing levels and frequencies affected for the KO rats compared to WT rats (Figure 3d). We found no effect of liraglutide treatment on estimated hearing levels. Although we observed statistically significant differences at 6.5 months of age in liraglutide-treated Wfs1 KO rats (from 2 kHz range) the obtained results serve minimal value (changes less than 10 dB in few individual frequencies). In summary, we found that Wfs1 KO rats lose hearing sensitivity around 6.5 months of age and liraglutide treatment was not able to ameliorate the decline from analyzed frequencies (Figure 3c).

#### **16-month treatment with liraglutide protects against vision loss in Wfs1 KO animals**

The complications in ophthalmic system in WS patients are described by decrease in visual acuity, constriction of the peripheral visual field and loss in color vision lead by optic disc and nerve atrophy (Seynaeve et al., 1994). We have revealed that Wfs1 KO rats display clear degenerative processes in ophthalmic system and late intervention with liraglutide. Treatment of 9-month-old animals can maintain already reduced visual acuity by delaying the progression of optic nerve atrophy and potentially regenerating effect of optic nerve fibres (Plaas et al., 2017; Seppa et al., 2021). Here, our aim was to investigate if life-long treatment with liraglutide can protect Wfs1 KO animals from vision loss.

The optomotor responses were measured at the age of 8.5-9; 12.5 and 17 months (Figure 4). Visual acuity, as measured by the optokinetic response, was lower in 8.5-month-old Wfs1 KO rats as compared to WT rats of the same age ( $p < 0.01$ ) (Figure 4a), and treatment with liraglutide prevented this decline ( $p < 0.001$ ) (Figure 4a). At the age of 12.5 and 17 months,

visual acuity of Wfs1 KO animals had steadily declined with age ( $p < 0.0001$ ) (Figure 4a) and this decline was completely rescued by liraglutide treatment ( $p < 0.0001$ ) (Figure 4a). Intraocular pressure did not differ between the experimental groups at any time point measured (Figure 4b). Cataract severity evaluated in 13- and 17-month-old animals, was increased at the age of 13 months in Wfs1 KO rats compared to WT littermates ( $p < 0.001$ ) (Figure 4c), but liraglutide treatment protected Wfs1 KO animals from developing cataract (Figure 4c). In conclusion, despite insulin supplementation, saline-treated Wfs1 KO animals progressively show visual decline from 8.5 months of age, yet 16-month treatment with liraglutide was effective in protecting Wfs1 KO animals against loss of visual loss.

### **16-month treatment with liraglutide protected against the development of optic nerve atrophy in Wfs1 KO animals**

To unravel the structural changes underlying the vision loss in WS rats, and the protective effect of liraglutide hereon, we next assessed optic nerve integrity and retinal ganglion cell survival. Transmission electron microscopy (TEM) on optic nerves revealed that the number of optic nerve axons per field of view (FOV) was increased ( $p < 0.05$ ) (Figure 5b) while axon size was decreased ( $p < 0.05$ ) (Figure 5d) in liraglutide-treated Wfs1 KO animals, compared to age-matched saline-treated Wfs1 KO rats. The number of optic nerve axons area per FOV remained relatively stable in saline- and liraglutide-treated WT rats (Figure 5c). Axon area per FOV was decreased ( $p < 0.001$ ), myelin area per FOV was not changed (Figure 5e), and hence the g-ratio (axon area divided by axon area plus myelin area) was lower ( $p < 0.001$ ) (Figure 5f), in saline-treated Wfs1 KO rats compared to WT littermates. These changes were rescued by the treatment with liraglutide.

Furthermore, electron microscopy analysis of degenerating optic nerve fibers in Wfs1 KO animals demonstrated several pathological features (Figure 5a). First, abnormalities in the

myelin sheath were observed, including both infoldings and outfoldings that typically occurred in large caliber fibers and which resulted in axonal compression. Axonal decompression due to abnormally expanded peri-axonal spaces was also seen. Second, degenerating axons appeared hypermyelinated and complete loss of axons resulted in remaining myelin bodies (Figure 5a). Third, severe cases of myelin lamellae decompaction were observable independently from axon caliber. Finally, additional pathological signs of axon degeneration included severe vacuolization and axoplasm filled with an amorphous, granular and dark material, in axons with various calibers. These results are consistent with those previously published by our group (Seppa et al., 2019, 2021). Semi-quantitative assessment of these observable pathological alterations in the myelin and axonal structure further confirmed that axonal pathology was significantly increased in saline-treated Wfs1 KO animals compared to WT animals ( $p < 0.01$ ) (Figure 5g). Treatment with liraglutide reduced the number of degenerating optic nerve fibers compared to saline-treated Wfs1 KO animals ( $p < 0.05$ ) (Figure 5g).

Previously we have seen a decrease in the volume of optic nerve in 15-month-old Wfs1 KO animals (Plaas et al., 2017). Here, *in vivo* MRI revealed that optic nerve volume was also decreased in saline-treated Wfs1 KO animals at the age of 17 months ( $p < 0.001$ ) (Figure 5k) and 16-month treatment with liraglutide protected the optic nerve from atrophy.

Additionally, retinal ganglion cell density was measured by counting Brn3a-positive cells on retinal flatmounts. We observed a considerable decrease in Brn3a positive cells in saline-treated Wfs1 KO animals compared to saline-treated WT control rats ( $p < 0.05$ ) (Figure 5l). Administration of liraglutide for 16-month rescued ganglion cell density in the Wfs1 KO rats ( $p < 0.01$ ) (Figure 5l) and had no effect on WT retinas (Figure 5l).

Altogether, TEM and MRI studies of optic nerve integrity and histological assessment of retinal ganglion cell survival indicate that early intervention and long-term treatment liraglutide treatment has neuroprotective effect on maintaining Wfs1 KO rat's optic nerve integrity.

## Discussion

Wolfram syndrome (WS) is an inherited condition that is associated with juvenile-onset insulin-dependent diabetes mellitus, diabetes insipidus, deafness and optic atrophy (de Heredia et al., 2013). Diagnosis of WS is usually made during adolescence when aforementioned core clinical signs of the syndrome become evident (Bueno et al., 2018; de Heredia et al., 2013). WS is a systemic degenerative disorder additionally comprising ataxia, behavioral and psychiatric disorders, apnea, hypogonadism, and renal malformations (Chausseot et al., 2011; de Heredia et al., 2013; Barrett et al., 1995; Urano, 2016). Prevalence, severity and appearance of symptoms seems to depend on genetic background and the location of the mutations rendering the non-functional WFS1 protein (Bueno et al., 2018; Chausseot et al., 2011; Duan et al., 2018; Wilf-Yarkoni et al., 2021). Treatment of WS is supportive and focused on the signs and symptoms present, and no cure is available. The only known treatment strategy that has been proven effective in reducing the diabetes component of the syndrome as well as providing some degree of neuroprotection in several animal models of WS and in human patients, is treatment with GLP1 receptor agonists (Kondo et al., 2018; Scully and Wolfsdorf, 2020). Indeed, our previous work in WS rats has established that preventive treatment with liraglutide has a protective effect against developing diabetes mellitus and ceases the progression of neurodegeneration by halting the development of optic atrophy and reducing neuroinflammation (Toots et al., 2018; Seppa et al., 2019, 2021). The aim of this study was to evaluate the efficacy of long-term GLP1 RA treatment in a rat model of WS. For this purpose, 2-months-old WS rats without any major WS symptoms were treated with liraglutide

(0,4mg/kg/day) up to the age of 18 months and changes in diabetes markers, visual acuity and hearing sensitivity were monitored *in vivo* during the course of the 16-month treatment period.

The first symptom of WS is considered insulin dependent diabetes and therefore we evaluated diabetes markers throughout the experiment. In the beginning of the treatment the blood glucose, insulin, c-peptide and glucagon levels were indifferent between genotype and treatment groups. By the age of 7.5 months, all of the saline-treated Wfs1 KO rats developed glucose intolerance. Progressing decline in beta-cell function in Wfs1 KO animals eventually led to insulin deficiency and hyperglycemia at the age of 11.5 months: a key feature of type 2 diabetes. Whereas Wfs1 KO animals receiving liraglutide could be divided into two distinct groups at 7.5 months of age with 63% of the cases responding to the treatment preventing the development of glucose intolerance. These two groups (glucose tolerant and intolerant, or responders and non-responders to liraglutide) of Wfs1 KO animals in the liraglutide treatment group, could be the result of developing tolerance to GLP-1 receptor agonist during repetitive administration. This phenomenon has been observed in rodents yet might not occur in humans given that chronic liraglutide administration has been shown to be as effective as acute administration (Sedman et al., 2017, 2020). It should be emphasized that during the experiment the administered dose of liraglutide remained constant: whether increasing the therapeutic dose to non-responding animals could have improved glucose metabolism remains obscure. Nevertheless, liraglutide-treated Wfs1 KO animals were able to secrete insulin and c-peptide and we observed no indication of hyperglucagonemia. Until this time point, the glycemic control and development of diabetes followed the result of our previous study (Toots et al., 2018). These findings suggest a sensitive timeframe in order to begin the treatment of diabetic phenotype as later intervention had minimal effect on diabetic markers in animals that had already developed glucose intolerance (Seppa et al., 2019).

Subsequently we observed increased fasting blood glucose levels in saline-treated Wfs1 KO animals at 11.5 months of age. In order to manage and subsequently minimize complications induced by hyperglycemia, animals in need received insulin from 11.5 months of age (Katsuda et al., 2015). By the age of 16 months, 90 % of saline-treated Wfs1 KO animals had developed hyperglycemia and needed supportive insulin administration. The prevalence of diabetes in WS rats at this age is rather parallel with observations in humans diagnosed with WS (de Heredia et al., 2013). Development of hyperglycemia in liraglutide-treated rats was evidently delayed. Notably, at the end of experiment only 55% of the Wfs1 KO animals in the liraglutide treatment group required supportive insulin treatment. In addition, the average daily insulin dose is significantly lower compared to Wfs1 KO animals indicating improved glycemic control. These findings are supported by the clinical data where GLP-1R agonists have been shown to improve and preserve beta-cell function in patients with type 2 diabetes (Degn et al., 2004; Harder et al., 2004). Thus, we can conclude that liraglutide treatment was able to prevent the onset of diabetes in 55% Wfs1 KO animals and delay the onset of diabetes in 45% Wfs1 KO animals.

Sensorineural hearing loss in WS patients is slowly progressing and is typically diagnosed at the age of 8 years, with 75% prevalence (Karzon et al., 2018). Hearing loss can begin from birth to adolescence and can range from severe to mild hearing loss that deteriorates over time (Barrett et al., 1995; de Heredia et al., 2013). As hearing loss has not been previously studied in a WS animal model, our aim was to determine whether WS rats develop hearing loss and whether liraglutide has an effect on it. Therefore, we used a non-invasive DPOAE analysis, which has been effective in identifying patients with sensorineural hearing loss (Abdala & Visser-Dumont, 2001). The DPOAE method was used to evaluate cochlear function throughout the experiment. At 2 months of age hearing sensitivity was indistinguishable between experimental groups. From 6.5 months hearing sensitivity in the range from 2 to 4 kHz started to rapidly decline in saline-treated Wfs1 KO animals and this decline is further exacerbated at

the age of 11 months and 17 months. Although we did not observe a positive effect of liraglutide treatment on hearing loss, our findings provide first evidence that *Wfs1* KO animals develop progressive low-frequency neurosensory hearing impairment. Furthermore, we observed the decline in the hearing sensitivity at frequencies that recapitulate observations in humans (Eiberg et al., 2006; Sun et al., 2011; Lesperance et al., 2003). As the frequency range of rat hearing (250 Hz to 80 kHz) has the greatest sensitivity occurring between 8 and 38 kHz, which is much higher than that found in humans (20 Hz to 20 kHz) (Escabi et al., 2019), it is unfortunate that the DPOAE method was unable to measure the frequency range between 8 and 38 kHz. Nevertheless, the auditory system of rats and humans shares several anatomical and physiological features (Escabi et al., 2019) and additionally the cochlea structures of rodents and primates displays strong expression of Wolframin in homologous compartments (Suzuki et al., 2018; Hilson et al., 2009). Thus, our results indicate that rats develop progressive low-frequency neurosensory hearing loss similarly to WS patients, and also position the *Wfs1* KO rat as a genetic animal model for studying progressive sensorineural hearing impairment.

Ophthalmologic manifestations occur in ~90% of WS patients with median age of 11 years (de Heredia et al., 2013; Hoekel et al., 2014). These include optic nerve atrophy, cataract, abnormal pupillary light reflexes, nystagmus, and deficiencies in visual field leading to progressive decrease of visual acuity and impairment in color vision (Barrett et al., 1997; Genis et al., 1997; Zmyslowska et al., 2018; Samara et al., 2020). Therefore, we evaluated the effect of liraglutide treatment on different levels in the visual pathway. In order to assess visual function, i.e. visual acuity, we performed the optomotor response test and observed a progressive decrease in visual acuity in the saline-treated *Wfs1* KO rats. Whereas treatment with liraglutide resulted in optomotor response values comparable to treated WT rats throughout the observed timeframe. Notably, as the optomotor response test is a behavioral measurement, the deficits in visual acuity of the saline-treated *Wfs1* KO could be caused by possible deficiencies in animal

behavioral parameters or general well-being (Pierre et al., 2004). We cannot exclude the decline in visual acuity in saline-treated Wfs1 KO rats by severe progression of cataract. Interestingly, insulin treatment of Wfs1 KO animals did not have inhibitory effect on cataract progression as described in streptozotocin-diabetic rats, suggesting different etiology (Coulter et al., 1986). Also, the development of cataract seems to be independent from IOP as we did not find significant changes or abnormalities in the IOP in all treatment groups. Nevertheless, liraglutide treatment of Wfs1 KO rats delays cataract progression and reduces the severity of lens opacification. Visual system integrity was further assessed by measuring the density of retinal ganglion cells. By counting Brn3a positive cells, we confirmed a severe decrease in retinal ganglion cells in saline-treated Wfs1 KO rat retinas correlating with results obtained by optomotor response test. It should be declared that we observe positive correlation between blood glucose levels and ganglion cell number. These results are in accordance with our previous observations, which showed that also short-term liraglutide treatment rescued ganglion cell density in Wfs1 KO rats (Seppa et al., 2019). Additionally, we found a consistent reduction of axonal area and number of axons in the optic nerve of Wfs1 deficient rats, accompanied by neuropathological signs of degeneration, ultimately resulting in optic nerve atrophy (Plaas et al., 2017; Seppa et al., 2019, 2021). In the current study, we observed that the treatment with liraglutide was able to halt this neurodegeneration. Hence, the current study confirms the neuroprotective effect of GLP1-R agonists in Wfs1 deficient rats and other models of neurodegenerative diseases (Gault & Hölscher, 2008; Maskery et al., 2020; Perry et al., 2007; Seppa et al., 2019, 2021). The preventative treatment before the onset of ocular pathology with liraglutide is crucial not only in avoiding the progression of optic nerve atrophy but also maintaining retinal ganglion cells density and avoiding severe cataracts in WS rat model.

In conclusion, we investigated the long-term effect of liraglutide treatment on diabetes, visual system function and integrity and hearing sensitivity. Administration of the GLP-1R agonist

liraglutide before the onset of WS symptoms offers great protection against WS progression. Results from current and previous studies indicate that preventive and long-term treatment postpones the development of glucose intolerance (opposed to late intervention) (Toots et al., 2018) and protects against vision loss (Seppa et al., 2019, 2021; current paper) in animal model of WS. Our results might predict possible GLP-1R agonist treatment outcomes in clinical studies on WS patients.

In conclusion, we investigated the long-term effect of liraglutide treatment on diabetes, visual system function and integrity and hearing sensitivity. Administration of the GLP-1R agonist liraglutide before the onset of WS symptoms offers great protection against disease progression by postponing the development of glucose intolerance (opposed to late intervention) (Toots et al., 2028) and protecting against vision loss (Seppa et al., 2019, 2020; current paper) in animal model of WS. Current study might provide predictive value in order to estimate GLP-1R agonist treatment outcomes in clinical studies on WS patients. Obtained results suggest that patients carrying pathogenic variants of *WFS1* should be diagnosed and treated before any clinical symptoms such as diabetes, loss of vision and deafness occur as it could delay syndrome progression and therefor improve the quality of life and increase the number of healthily lived years.

## **Declarations**

### **Ethics approval and consent to participate**

Not applicable.

### **Consent for publication**

Not applicable.

## **Availability of data and materials**

Please contact author for data requests.

## **Funding**

This study was sponsored by Eye Hope Foundation iVZW, Damme, Belgium ([www.eyehopefoundation.org](http://www.eyehopefoundation.org)), by grant PSG471 (M.P.) from the Estonian Research Council, and by a grant from the Central Europe Leuven Strategic Alliance (CELSA/20/009). LDG is a senior postdoctoral research fellow of Research Foundation Flanders (FWO). Funding bodies had no role in the design of the study and interpretation of results.

## **Competing interests**

The authors declare that they have no competing interests.

## **Authors' contributions**

Ma.Pl. conceived and directed the study. Ma.Pl., A.T., K.S. and T.J. designed the experiments. Ma.Pl., R.R., A.T., T.J., Ma.Pa., and K.S. performed animal experiments. Ma.Pa. performed the cataract scoring and corresponding data interpretation. Mi.Pl. performed hearing evaluation data analysis and interpretation. K.S. conducted MRI experiments. K.S., KGK., M.A.H. performed the analysis of MRI data. L.D.G. and L.M. performed the retinal whole-mount immunohistochemical staining, corresponding data analysis and interpretation. T.J. and Ma.Pl. performed electron microscopy on optic nerves and corresponding data analysis. T.J., Ma.Pl., K.S., L.D.G., L.M., A.K., E.V. helped to draft and substantively revise the manuscript. All authors read and approved the final version of the manuscript.

## **Acknowledgements**

Not applicable.

## Footnotes

Tissues are available for collaborative studies - investigators interested in collaborating should contact directly with corresponding author of this paper.

## Figures

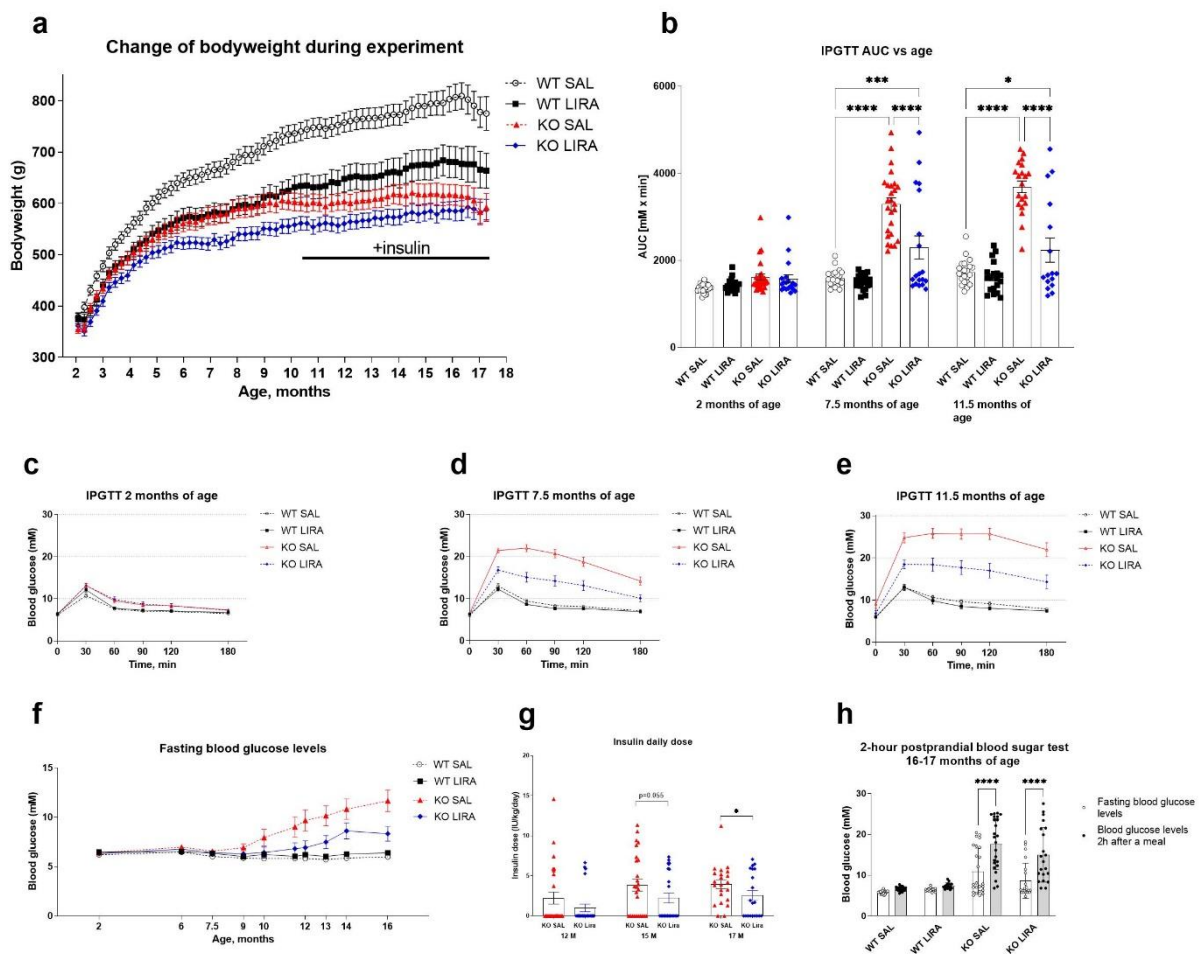


**Figure 1. A 16-month treatment with liraglutide delays the onset of diabetes in a rat model of Wolfram syndrome. (a)** Body weight change over 16 months of liraglutide treatment. For intraperitoneal glucose tolerance tests (IPGTTs), blood glucose levels were measured after administration of glucose (2 g/kg i.p.), and the area under the curve (AUC) was calculated. **(b)** IPGTT AUC at the age of 2, 7.5 and 11.5 months. Liraglutide treatment delays the progression of glucose intolerance in *Wfs1* KO rats. **(b)** Visually, the animals in the KO LIRA group are divided into two groups, one group with glucose tolerance similar to that of WT SAL animals and the second group with animals similar to that of KO SAL. The data were compared using two-way ANOVA followed by Tukey's multiple comparisons test. The data

are presented as the mean  $\pm$  SEM, \* $p$  < 0.05, \*\*\* $p$  < 0.001, \*\*\*\* $p$  < 0.0001,  $n$  = 16–27 per group. IPGTT at the age of (c) 2, (d) 7.5 and (e) 11.5 months. (f) Fasting blood glucose levels during 16-month treatment. (g) Insulin daily dose at 12, 15 and 17 months of age, the data were compared using one-tailed unpaired t-test. The data are presented as the mean  $\pm$  SEM, \* $p$  < 0.05,  $n$  = 24–27 per group. For 2-hour postprandial blood sugar tests, blood glucose levels were measured after 3 hours of fasting and then blood glucose was measured 2 hours after the animals had access to food. (h) Blood glucose levels from 2-hour postprandial blood sugar test at the age of 16-17 months, the data were compared using repeated measures ANOVA followed by Bonferroni's multiple comparisons test. The data are presented as the mean  $\pm$  SEM, \*\*\*\* $p$  < 0.0001,  $n$  = 21–24 per group.

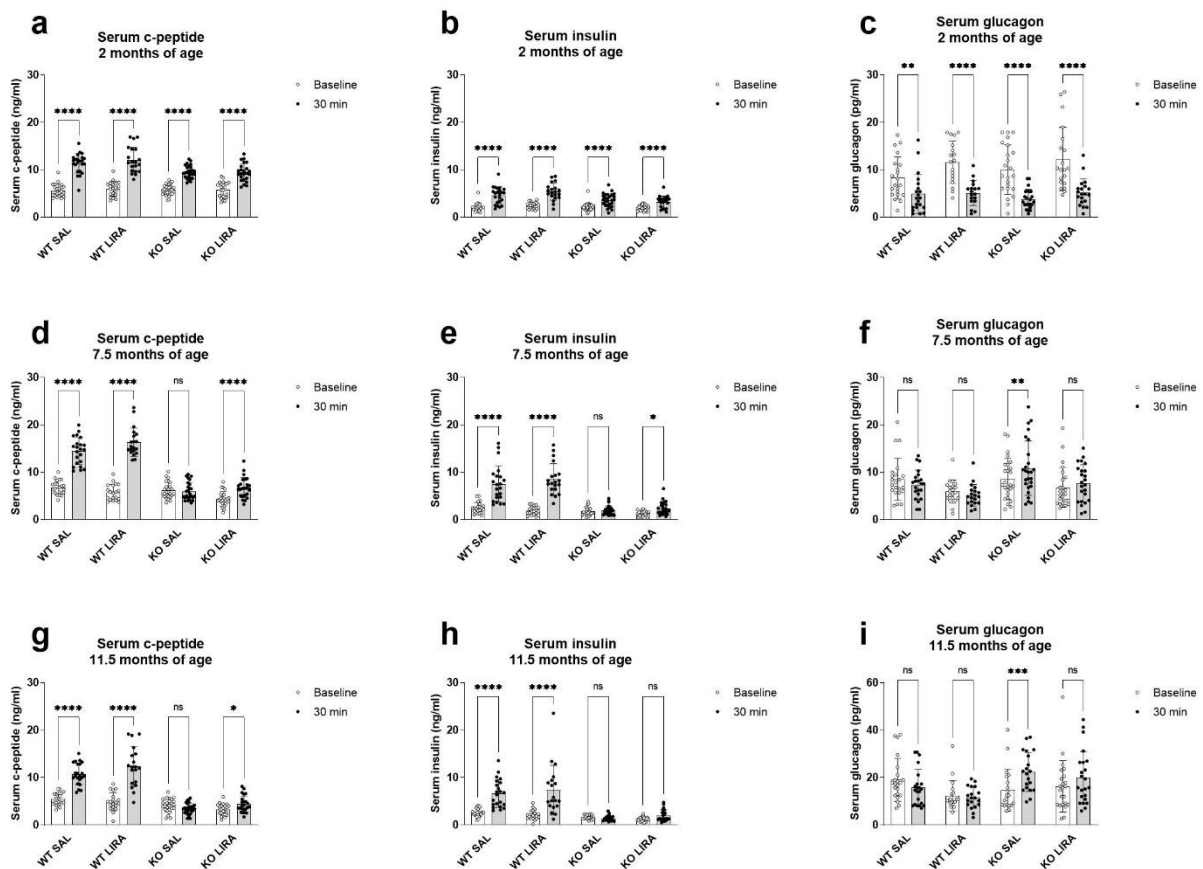


**Figure 2. Prolonged treatment with liraglutide maintains c-peptide secretion until the age of 11 months and thereby delays the development of diabetes in a rat model of Wolfram syndrome.** At the age of 2, 7.5 and 11.5 months, serum (a, d, g) c-peptide, (b, e, h) insulin and (c, f, i) glucagon levels before and 30 minutes after administration of glucose in the glucose tolerance test (IPGTT). (a, b, c) At the age of 2 months, there were no differences between experimental groups. At the age of 7.5 months, *Wfs1* KO rats show the first signs of diabetes, i.e. reduced (d) c-peptide and (e) insulin levels, and increased (f) glucagon levels after glucose administration. Liraglutide treatment prevented these changes

and at the age of 11.5 months, liraglutide-treated Wfs1 KO rats were still able to secrete (g) c-peptide. The data were compared using repeated measures ANOVA followed by Bonferroni's multiple comparisons test. The data are presented as the mean  $\pm$  SEM, non-significant (ns), \* $p < 0.05$ , \*\* $p < 0.01$ , \*\*\* $p < 0.001$ , \*\*\*\* $p < 0.0001$ ,  $n = 20-27$  per group.

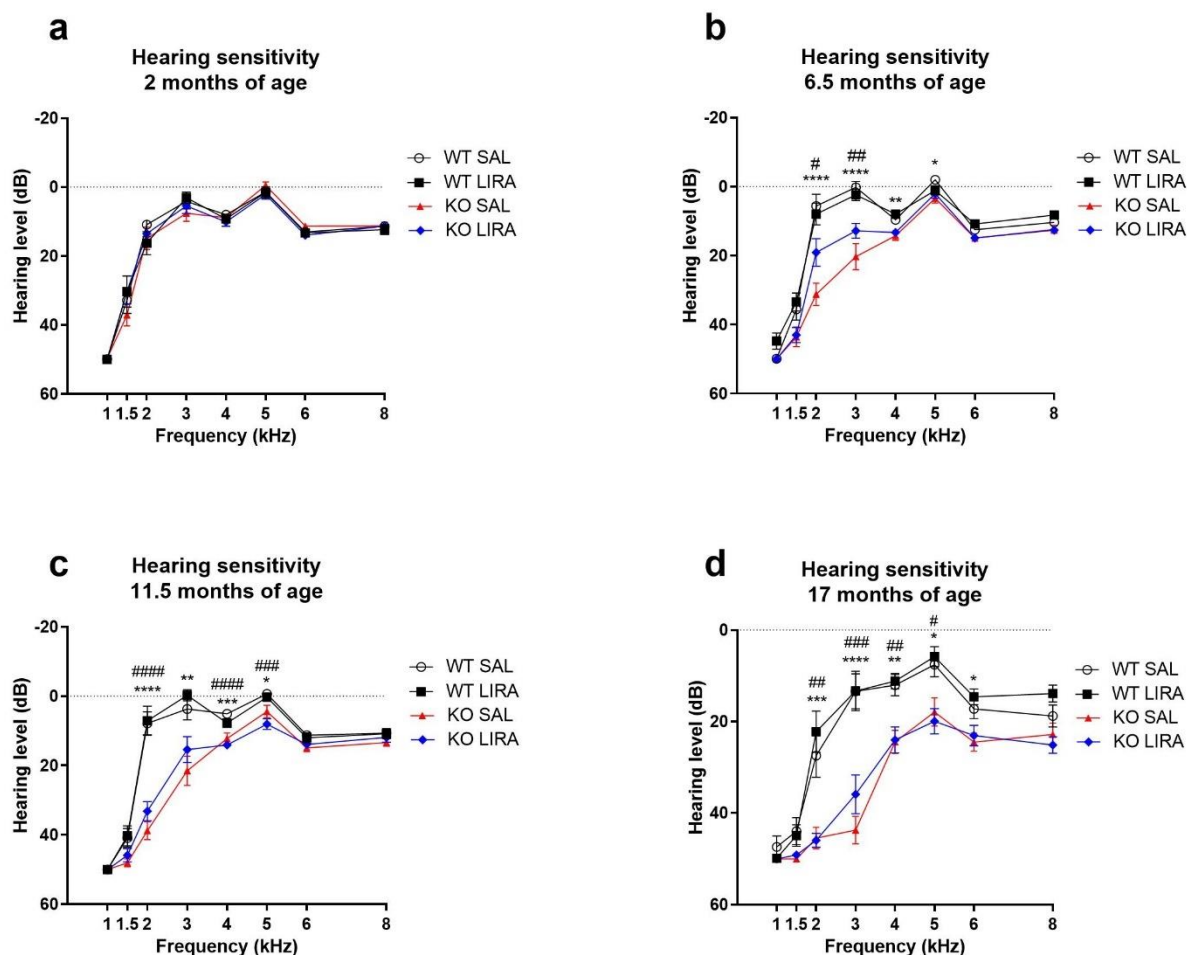
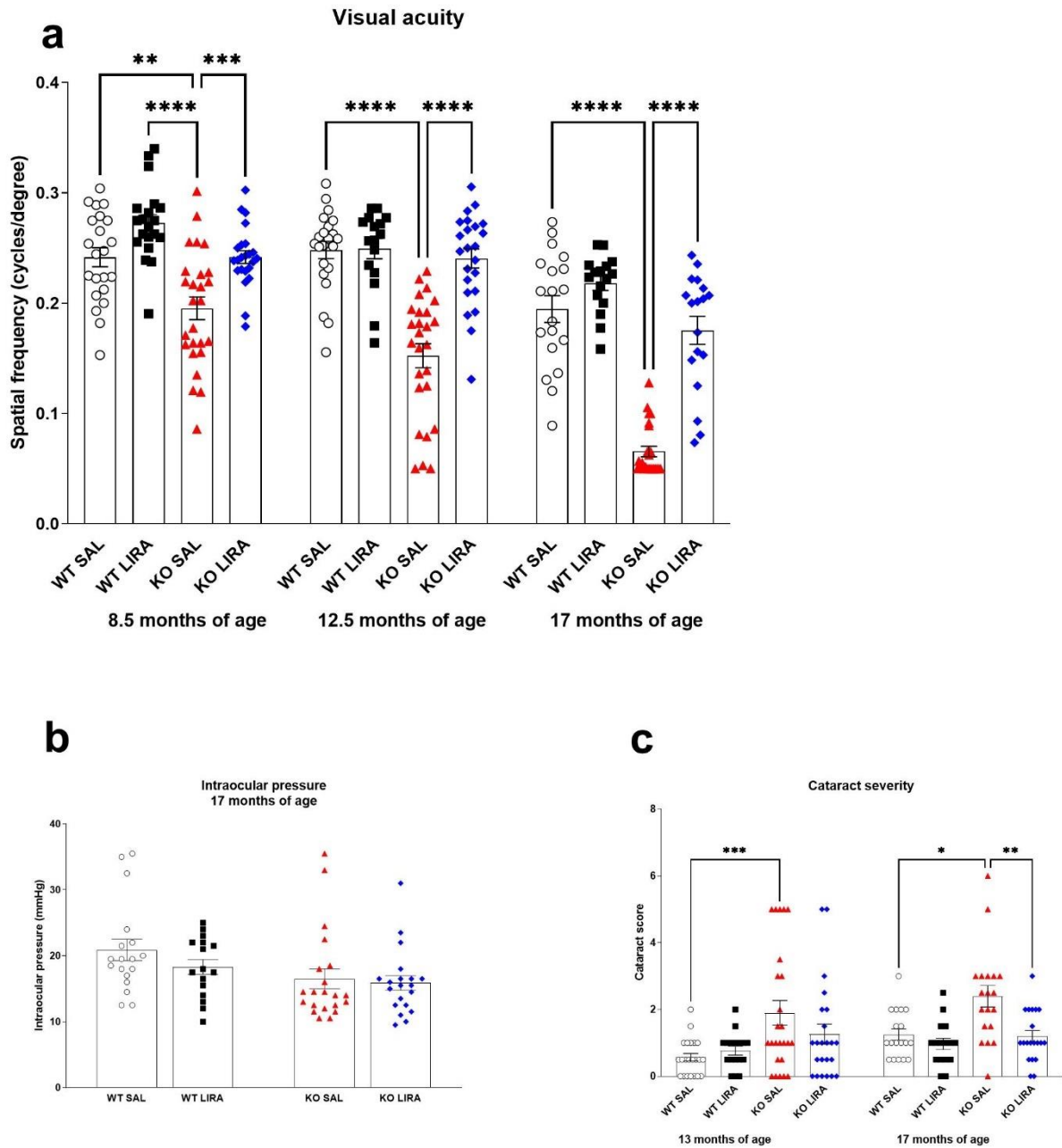
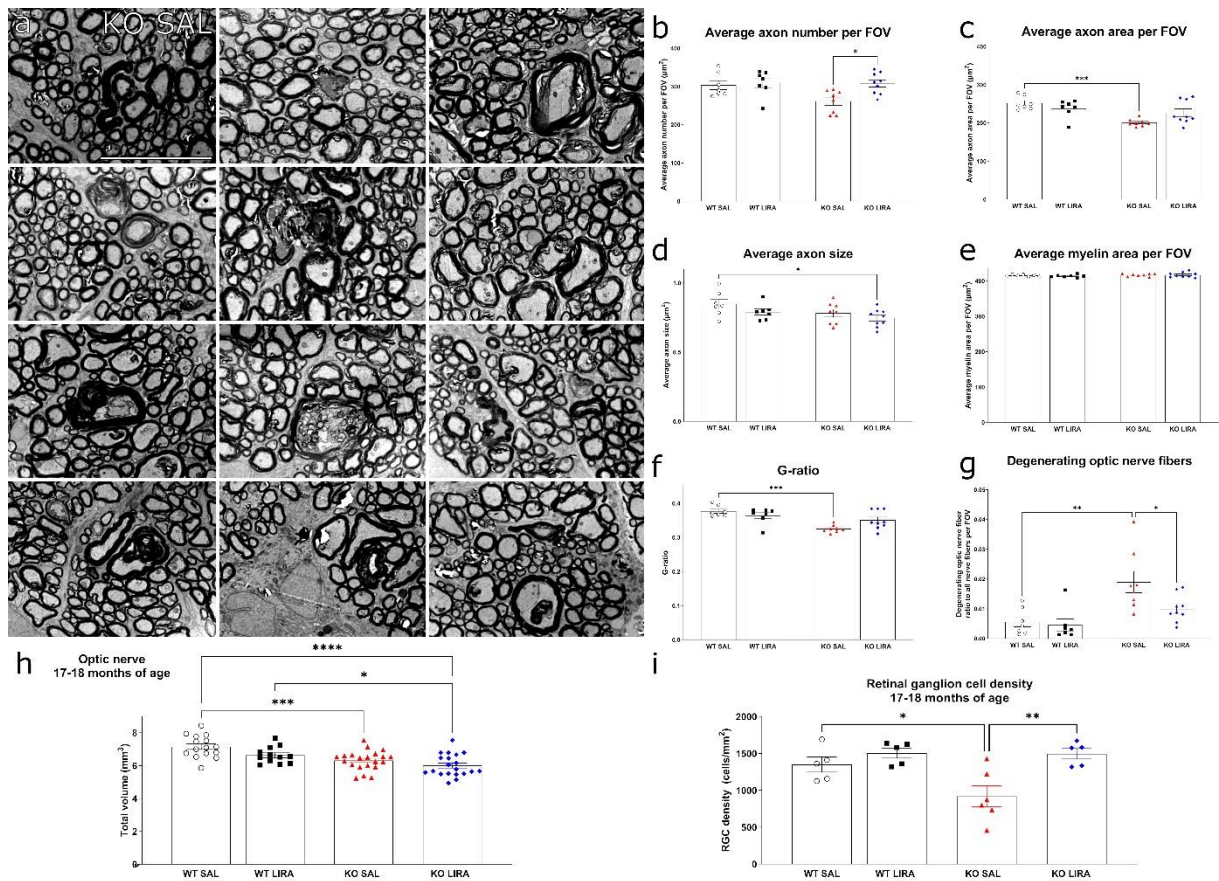


Figure 3. At the age of 6.5 months, hearing sensitivity of Wfs1 KO rats starts to decline in the range of 2 to 4 kHz and liraglutide treatment delays the decline of hearing sensitivity. Hearing sensitivity was measured for both ears and the data were averaged. Hearing sensitivity at (a) 2; (b) 6.5; (c) 11 and (d) 17 months of age. (a) At the age of 2 months, hearing sensitivity is similar for all animals regardless of treatment group and genotype. (b) At the age of 6.5 months hearing sensitivity of Wfs1 KO rats starts to decline in the range of 2 to 4 kHz, this decline is further exacerbated at the age of (c) 11 months and (d) 17 months. (b) Liraglutide delays the decline of hearing sensitivity. However, liraglutide treatment does not prevent from the decline of hearing sensitivity in older Wfs1 KO rats (c-d). The data were compared using one-way ANOVA followed by Tukey's HSD tests. The data are presented as the mean  $\pm$  SEM. Significance was measured between genotype and treatment. \*  $p < 0.05$ , \*\* $p < 0.01$ , \*\*\* $p < 0.001$ , \*\*\*\* $p < 0.0001$  WT SAL compared to KO SAL, #  $p < 0.05$ , ## $p < 0.01$ , ### $p < 0.001$ , #### $p < 0.0001$  WT SAL compared to KO LIRA,  $n = 15-26$ .



**Figure 4. A 16-month treatment with GLP1 receptor agonist liraglutide protects against vision loss in a rat model of Wolfram syndrome. (a) Optokinetic reflex response at the age of 8.5, 12.5 and 17 months. Response was measured for both eyes and the data were averaged. In KO SAL animals, visual acuity decreased over time, while in KO LIRA animals, visual acuity stayed at the same level with WT SAL animals. (b) Intraocular pressure at the age of 17 months was unchanged between experimental groups. (c) Cataract severity at the age of 13 and 17 months. The data were compared using two-way ANOVA followed by Tukey's multiple comparisons test. The data are presented as the mean  $\pm$  SEM, \* $p < 0.05$ , \*\* $p < 0.01$ , \*\*\* $p < 0.001$ , \*\*\*\* $p < 0.0001$ ,  $n = 16-24$  per group.**





**Figure 5. Morphometric analyzes of optic nerve and evaluation of ganglion cell density. (a) electron micrographs representing pathological manifestations of KO rat's optic nerves. Large caliber optic nerve fibers display: axonal loss resulting in myelin compression; electron-dense axoplasm accompanied by demyelination; myelin lamina decompaction; axonal loss accompanied by myelin decompaction; severe myelin compaction followed by axon compression; axons of large caliber display severe vacuolization; axonal compression hyper-myelinated fibers; infoldings of myelin sheet resulting in axonal compression and subsequent degeneration; large fibers display widening of peri-axonal space and inversion of myelin sheet. (b-i) graphs displaying measurements of: (b) average number of axons per field of view (FOV); (c) average area of axons ( $\mu\text{m}^2$ ) per field of view (FOV); (d) average axon cross-section area (e) average myelin area ( $\mu\text{m}^2$ ) per FOV; (f) area based G-ratio (axon area divided by axon area plus myelin area); (g) ratios of degenerating fibers calculated as the ratio of degenerating fibers to all counted fibers per FOV,  $n = 7-9$  per group. (h) Volume of optic nerve obtained by analyzing MRI data at 17-18 months of age,  $n = 12-21$  per group. (i) Graph displays retinal ganglion cell density at the end of the experiment, at the age of 17-18 months,  $n = 5-6$  per group. Quantitative data were compared one-way ANOVA followed by Tukey's multiple comparisons test. The data are presented as the mean  $\pm$  SEM, \* $p < 0.05$ , \*\* $p < 0.01$ , \*\*\* $p < 0.001$ .**

## References

Pathme GmbH Whitepaper: [cited 2021 Sep 13]. Available from: [https://www.pathme.de/download/whitepapers/Whitepaper\\_Short\\_RelationBetweenDPOAEs\\_and\\_behavioural\\_pure\\_tone\\_threshold.pdf](https://www.pathme.de/download/whitepapers/Whitepaper_Short_RelationBetweenDPOAEs_and_behavioural_pure_tone_threshold.pdf)

Abdala C, Visser-Dumont L. Distortion product otoacoustic emissions: A tool for hearing assessment and scientific study. *Volta Rev.* 2001;103(4):281–302.

Barrett T., Bunday S. E. MAF. ( DIDMOAD ) syndrome UK nationwide study of Wolfram. *Lancet.* 1995;346:1458–63.

Barrett TG, Bunday SE. Wolfram (DIDMOAD) syndrome. *J Med Genet.* 1997;34(10):838–41.

Bonnet Wersinger D, Benkafadar N, Jagodzinska J, Hamel C, Tanizawa Y, Lenaers G, et al. Impairment of visual function and retinal ER stress activation in *Wfs1*-deficient mice. *PLoS One.* 2014;9(5).

Bueno GE, Ruiz-Castañeda D, Martínez JR, Muñoz MR, Alascio PC. Natural history and clinical characteristics of 50 patients with Wolfram syndrome. *Endocrine* [Internet]. 2018;61(3):440–6. Available from: <https://doi.org/10.1007/s12020-018-1608-2>

Cagalinec M, Liiv M, Hodurova Z, Hickey MA, Vaarmann A, Mandel M, et al. Role of Mitochondrial Dynamics in Neuronal Development: Mechanism for Wolfram Syndrome. *PLoS Biol.* 2016;14(7):1–28.

Chandra M, Riley MGI, Johnson DE. Spontaneous Neoplasms in Aged Sprague-Dawley Rats. *Toxicol Pathol.* 1992;20:327–40.

Chaussonot A, Bannwarth S, Rouzier C, Vialettes B, Mkaem SA El, Chabrol B, et al. Neurologic features and genotype-phenotype correlation in Wolfram syndrome. *Ann Neurol* [Internet]. 2011;69(3):501–8. Available from: <http://www.hgvs.org/>

Coulter JB, Eaton DK, Marr LK. Effects of diabetes and insulin treatment on sorbitol and water of rat lenses. *Ophthalmic Res*. 1986;18(6):357–62.

De Heredia ML, Clèries R, Nunes V. Genotypic classification of patients with Wolfram syndrome: Insights into the natural history of the disease and correlation with phenotype. Vol. 15, *Genetics in Medicine*. 2013. p. 497–506.

Degn KB, Juhl CIB, Sturis J, Jakobsen G, Brock B, Chandramouli V, et al. One Week 's Treatment With the Long-Acting Glucose Release in Patients with Type 2 Diabetes. *Diabetes*. 2004;53(10):1187–94.

Delprat B, Maurice T, Delettre C. Wolfram syndrome: MAMs' connection? review-article. *Cell Death Dis*. 2018;9(3).

Duan L, Li Q, Tong AL, Mao JF, Yu M, Yuan T, et al. Clinical characteristics of wolfram syndrome in Chinese population and a novel frameshift mutation in WFS1. *Front Endocrinol (Lausanne)* [Internet]. 2018;9(FEB):18. Available from: [www.frontiersin.org](http://www.frontiersin.org)

Eiberg H, Hansen L, Kjer B, Hansen T, Pedersen O, Bille M, et al. Autosomal dominant optic atrophy associated with hearing impairment and impaired glucose regulation caused by a missense mutation in the WFS1 gene. *J Med Genet* [Internet]. 2006;43:435–40. Available from: [www.jmedgenet.com](http://www.jmedgenet.com)

Escabi CD, Frye MD, Trevino M, Lobarinas E. The rat animal model for noise-induced hearing loss. *J Acoust Soc Am*. 2019;146(5):3692–709.

Fonseca SG, Fukuma M, Lipson KL, Nguyen LX, Allen JR, Oka Y, et al. WFS1 is a novel component of the unfolded protein response and maintains homeostasis of the endoplasmic reticulum in pancreatic  $\beta$ -cells. *J Biol Chem* [Internet]. 2005;280(47):39609–15. Available from: <http://dx.doi.org/10.1074/jbc.M507426200>

Gault VA, Hölscher C. GLP-1 agonists facilitate hippocampal LTP and reverse the impairment of LTP induced by beta-amyloid. *Eur J Pharmacol*. 2008;587(1–3):112–7.

Geeraerts E, Dekeyster E, Gaublomme D, Salinas-Navarro M, De Groef L, Moons L. A freely available semi-automated method for quantifying retinal ganglion cells in entire retinal flatmounts. *Exp Eye Res* [Internet]. 2016;147:105–13. Available from: <http://dx.doi.org/10.1016/j.exer.2016.04.010>

Genís D, Dávalos A, Molins A, Ferrer I. Wolfram syndrome: A neuropathological study. *Acta Neuropathol*. 1997;93(4):426–9.

Gharanei S, Zatyka M, Astuti D, Fenton J, Sik A, Nagy Z, et al. Vacuolar-type H<sup>+</sup>-ATPase V1A subunit is a molecular partner of Wolfram syndrome 1 (WFS1) protein, which regulates its expression and stability. *Hum Mol Genet*. 2013;22(2):203–17.

Hansen G, Jelsing J, Vrang N. Effects of liraglutide and sibutramine on food intake, palatability, body weight and glucose tolerance in the gubra DIO-rats. *Acta Pharmacol Sin* [Internet]. 2012;33:194–200. Available from: [www.chinaphar.com](http://www.chinaphar.com)

Harder H, Mscodont NL, Thi TDT, Astrup A. The Effect of Liraglutide, a Long-Acting 24-h Energy Expenditure in Patients Glycemic Control, Body Composition, and Glucagon-Like Peptide 1 Derivative, on With Type 2 Diabetes. *Diabetes Care*. 2004;27(8):1915–21.

Hilson JB, Merchant SN, Adams JC, Joseph JT. Wolfram syndrome: A clinicopathologic correlation. *Acta Neuropathol.* 2009;118(3):415–28.

Hoekel J, Chisholm SA, Al-Lozi A, Hershey T, Earhart G, Hullar T, et al. Ophthalmologic correlates of disease severity in children and adolescents with Wolfram syndrome. *J AAPOS.* 2014;18(5):461-465.e1.

Karzon R, Narayanan A, Chen L, Lieu JEC, Hershey T. Longitudinal hearing loss in Wolfram syndrome. *Orphanet J Rare Dis [Internet].* 2018 [cited 2021 Jun 10];13(102). Available from: <https://doi.org/10.1186/s13023-018-0852-0>

Katsuda Y, Sasase T, Tadaki H, Mera Y. Contribution of hyperglycemia on diabetic complications in obese type 2 diabetic SDT fatty rats : effects of SGLT inhibitor phlorizin. *Exp Anim.* 2015;64(November 2014):161–9.

Kemp DT. Stimulated acoustic emissions from within the human auditory system. *J Acoust Soc Am.* 1978;64(5):1386–91.

Kemp DT. Otoacoustic emissions, their origin in cochlear function, and use. *Br Med Bull.* 2002;63:223–41.

Kondo M, Tanabe K, Amo-Shiinoki K, Hatanaka M, Morii T, Takahashi H, et al. Activation of GLP-1 receptor signalling alleviates cellular stresses and improves beta cell function in a mouse model of Wolfram syndrome. *Diabetologia.* 2018;61(10):2189–201.

Larsen PJ, Fledelius C, Knudsen LB, Tang-Christensen M. Systemic Administration of the Long-Acting GLP-1 Derivative NN2211 Induces Lasting and Reversible Weight Loss in Both Normal and Obese Rats. *Diabetes.* 2001;50(7–12):2530–9.

Lesperance MM, Hall JW, San Agustin TB, Leal SM. Mutations in the Wolfram syndrome type 1 gene (WFS1) define a clinical entity of dominant low-frequency sensorineural hearing loss. *Arch Otolaryngol - Head Neck Surg* [Internet]. 2003;129(4):411–20. Available from: <https://jamanetwork.com/>

Livesey JC, Wiens LW, von Seggern DJ, Barlow WE, Arnold A. Inhibition of Radiation Cataractogenesis by WR-77913. *Radiat Res*. 2014;141(1):99–104.

Luippold G, Bedenik J, Voigt A, Grempler R. Short-and Longterm Glycemic Control of Streptozotocin-Induced Diabetic Rats Using Different Insulin Preparations. *PLoS One* [Internet]. 2016;11(6). Available from: [www.idf.org](http://www.idf.org)

Luuk H, Koks S, Plaas M, Hannibal J, Rehfeld JF, Vasar E. Distribution of Wfs1 protein in the central nervous system of the mouse and its relation to clinical symptoms of the Wolfram syndrome. *J Comp Neurol*. 2008;509(6):642–60.

Maskery MP, Holscher C, Jones SP, Price CI, Strain WD, Watkins CL, et al. Glucagon-like peptide-1 receptor agonists as neuroprotective agents for ischemic stroke: a systematic scoping review. Vol. 41, *Journal of Cerebral Blood Flow and Metabolism*. 2021. p. 14–30.

Nadal-Nicolás FM, Jiménez-López M, Sobrado-Calvo P, Nieto-López L, Cánovas-Martinez I, Salinas-Navarro M, et al. Brn3a as a marker of retinal ganglion cells: Qualitative and quantitative time course studies in naïve and optic nerve-injured retinas. *Investig Ophthalmol Vis Sci*. 2009;50(8):3860–8.

Nordquist L, Sjöquist M. Improvement of insulin response in the streptozotocin model of insulin-dependent diabetes mellitus. Insulin response with and without a long-acting insulin treatment. *Animal*. 2009 May 1;3(5):685–9.

Perry TA, Holloway HW, Weerasuriya A, Mouton PR, Duffy K, Mattison JA, et al. Evidence of GLP-1-mediated neuroprotection in an animal model of pyridoxine-induced peripheral sensory neuropathy. *Exp Neurol*. 2007;203(2):293–301.

Pierre C, Serge P, Raymond R, Johan A, Jose S. The optomotor response : A robust first-line visual screening method for mice. *Vision Res*. 2005;45(11):1439–46.

Plaas M, Seppa K, Reimets R, Jagomäe T, Toots M, Koppel T, et al. Wfs1-deficient rats develop primary symptoms of Wolfram syndrome: Insulin-dependent diabetes, optic nerve atrophy and medullary degeneration. *Sci Rep*. 2017;7(1):1–16.

Rigoli L, Lombardo F, Di Bella C. Wolfram syndrome and WFS1 gene. *Clin Genet*. 2011;79(2):103–17.

Samara A, Lugar HM, Hershey T, Shimony JS. Longitudinal assessment of neuroradiologic features in wolfram syndrome. *Am J Neuroradiol*. 2020;41(12):2364–9.

Schindelin J, Arganda-Carrera I, Frise E, Verena K, Mark L, Tobias P, et al. Fiji - an Open platform for biological image analysis. *Nat Methods*. 2009;9(7).

Scully KJ, Wolfsdorf JI. Efficacy of GLP-1 Agonist Therapy in Autosomal Dominant WFS1-Related Disorder: A Case Report. *Horm Res Paediatr*. 2021;93(6):409–14.

Sedman T, Krass M, Rünkorg K, Vasar E, Volke V. Tolerance develops toward GLP-1 receptor agonists' glucose-lowering effect in mice. *Eur J Pharmacol [Internet]*. 2020;885(June):173443.

Available from: <https://doi.org/10.1016/j.ejphar.2020.173443>

Sedman T, Krass M, Rünkorg K, Vasar E, Volke V. Tolerance develops toward GLP-1 receptor agonists ' glucose-lowering effect in mice. *Eur J Pharmacol* [Internet]. 2020;885(August):173443. Available from: <https://doi.org/10.1016/j.ejphar.2020.173443>

Seppa K, Jagomäe T, Kukker KG, Reimets R, Pastak M, Vasar E, et al. Liraglutide, 7,8-DHF and their co-treatment prevents loss of vision and cognitive decline in a Wolfram syndrome rat model. *Sci Rep* [Internet]. 2021;11(1):1–14. Available from: <https://doi.org/10.1038/s41598-021-81768-6>

Seppa K, Toots M, Reimets R, Jagomäe T, Koppel T, Pallase M, et al. GLP-1 receptor agonist liraglutide has a neuroprotective effect on an aged rat model of Wolfram syndrome. *Sci Rep*. 2019;9(1):1–13.

Seynaeve H, Vermeiren A, Leys A, Dralands L. Four cases of Wolfram syndrome: ophthalmologic findings and complications. *Bull Soc Belge Ophtalmol*. 1994;252:75–80.

Sheppard AM, Zhao DL, Salvi R. Isoflurane anesthesia suppresses distortion product otoacoustic emissions in rats. *J Otol* [Internet]. 2018;13(2):59–64. Available from: <https://doi.org/10.1016/j.joto.2018.03.002>

Strom TM, Hörtnagel K, Hofmann S, Gekeler F, Scharfe C, Rabl W, et al. Diabetes insipidus, diabetes mellitus, optic atrophy and deafness (DIDMOAD) caused by mutations in a novel gene (wolframin) coding for a predicted transmembrane protein. *Hum Mol Genet*. 1998;7(13):2021–8.

Sun Y, Cheng J, Lu Y, Li J, Lu Y, Jin Z, et al. Identification of two novel missense WFS1 mutations, H696Y and R703H, in patients with non-syndromic low-frequency sensorineural hearing loss. *J Genet Genomics*. 2011;38(2):71–6.

Suzuki N, Hosoya M, Oishi N, Okano H, Fujioka M, Ogawa K. Expression pattern of wolframin, the WFS1 (Wolfram syndrome-1 gene) product, in common marmoset (*Callithrix jacchus*) cochlea. *Neuroreport*. 2016;27(11):833–6.

Takei D, Ishihara H, Yamaguchi S, Yamada T, Tamura A, Katagiri H, et al. WFS1 protein modulates the free Ca<sup>2+</sup> concentration in the endoplasmic reticulum. *FEBS Lett*. 2006;580(24):5635–40.

Toots M, Seppa K, Jagomäe T, Koppel T, Pallase M, Heinla I, et al. Preventive treatment with liraglutide protects against development of glucose intolerance in a rat model of Wolfram syndrome. *Sci Rep*. 2018;8(1):1–10.

Urano F. Wolfram Syndrome: Diagnosis, Management, and Treatment. Available from: <http://wolframsyndrome.dom.wustl.edu/>

Wilf-Yarkoni A, Shor O, Fellner A, Hellmann MA, Pras E, Yonath H, et al. Mild Phenotype of Wolfram Syndrome Associated With a Common Pathogenic Variant Is Predicted by a Structural Model of Wolframin. *Neurol Genet*. 2021;7(2):e578.

Zmyslowska A, Waszczykowska A, Baranska D, Stawiski K, Borowiec M, Jurowski P, et al. Optical coherence tomography and magnetic resonance imaging visual pathway evaluation in Wolfram syndrome. *Dev Med Child Neurol*. 2019;61(3):359–65.